APEM journal
Advances in Production Engineering & Management
Volume 15 | Number 1 | March 2020 | pp 5–17
https://doi.org/10.14743/apem2020.1.345
ISSN 1854-6250
Journal home: apem-journal.org
Original scientific paper

Neuro-mechanistic model for cutting force prediction in helical end milling of metal materials layered in multiple directions

Zuperl, U.[a,*], **Cus, F.**[a], **Zawada-Tomkiewicz, A.**[b], **Stępień, K.**[c]

[a]University of Maribor, Faculty of Mechanical Engineering, Slovenia
[b]Koszalin University of Technology, Department of Mechanical Engineering, Poland
[c]Kielce University of Technology, Faculty of Mechatronics and Mechanical Engineering, Poland

ABSTRACT

In machining of multi-layer metal materials used frequently for the manufacture of transfer sheet-metal forming tools, the cutting edge is often damaged because of cutting force peaks. Therefore, a neuro-mechanistic model, presented in this paper, has been created for accurate prediction of cutting forces in helical end milling of multidirectional layered materials. The generalized model created takes into account the complex geometry of the helical end milling cutter, the instantaneous chip thickness and the direction of depositing of the individual layer of the multidirectional layered material considered in the calculation through predicted specific cutting forces. For the prediction of specific cutting forces for individual layers a neural network is incorporated in the model. The comparison with experimental data shows that the model predicts accurately the flow of cutting force in milling of multidirectional layered metal materials for any combination of cutting parameters, tool engagement angle and directions of depositing three layers of material. The predicted cutting force values agree well with the values obtained, the maximum error of predicted cutting forces is 16.1 % for all comparison tests performed.

ARTICLE INFO

Keywords:
Helical end milling;
Multidirectional layered metal material;
Cutting forces;
Specific cutting forces;
Neuro-mechanistic model;
Modelling;
Prediction;
Artificial neural networks

**Corresponding author:*
uros.zuperl@um.si
(Zuperl, U.)

Article history:
Received 18 April 2019
Revised 16 March 2020
Accepted 23 March 2020

1. Introduction

Tool shops making resistant transfer sheet-metal forming tools use the most up-to-date multi-layer metal materials. The materials are made layer after layer by the LENS (laser engineered net shaping) process [1].

In the multi-layer material, the individual layers are deposited in different directions, therefore the machinability of the layered material is changing from layer to layer. Machinability also depends on the angle between the feeding axis of the tool and direction of layer depositing.

Machining of such materials is a demanding operation requiring continuous adaption of machining parameters to momentary cutting conditions. A review of literature identifies no researches in the field of machinability of multidirectional layered metal materials. There are a few researches on machinability of difficult-to-machine nickel-based alloys [2], titanium alloys [3] and composite materials [4]. M'Saoubi *et al.* [5] presented an overview of the recent advances in high performance cutting of aerospace alloys and composite used in aeroengine and aero structure applications.

Hojati *et al*. [6] and Bonati *et al*. [7] examined the machinability of additively manufactured Ti6Al4V alloy parts in the micro-milling with a particular emphasis on cutting forces. They found out that the microstructure of the material, in addition to the hardness of the material, has a significant impact on the cutting forces. Furthermore, the cutting forces for additively manufactured part are lower than those of standard manufactured part despite of their higher hardness. Montevecchi *et al*. [8] analysed cutting forces in order to examine the machinability of AISI H13 alloy. Mechanistic approach was employed to identify cutting force coefficients and to investigate the behaviour of the cutting force for laser deposition (LENS). Results outlined that the additively manufactured AISI H13 material had reduced machinability compared to the same standard material at wrought state.

In machining multi-layer metal materials high cutting force peaks and excessive wear and extensive damages of the cutting tool occur because of the non-uniform shape of chips [5]. The cutting force frequencies measured in milling can be directly associated with the manner of chip formation [9]. Also the roughness of the machined surface depends strongly on the manner of chip formation and is in correlation with cutting force. The tool wear and damages are directly associated with cutting forces, therefore accurate prediction and monitoring of cutting forces is a key factor assuring quality of machining. By the cutting forces, accurately predicted, the quality of machining can be evaluated and undesirable effects on the cutting tool reduced [10].

Literature comprises a lot of researches on modeling of cutting forces in oblique cutting. The majority of cutting force models for oblique cutting are created by the mechanistic modelling technique [9]. The developed mechanistic models for oblique cutting in predicting of cutting forces take into account: radial cutter runout [11]; tool deflection [12]; system dynamics and flank wear [9]; indentation of the cutting edge into the work material [13]; dynamic chip thickness, chip forming and friction forces [14]; radius of curvature for sculptured surface machining [15]; Johnson-Cook constitutive equation [16].

In the mechanistic models, the cutting forces are associated with instantaneous uncut chip thickness through experimentally defined specific cutting forces [17]. The principal challenge in creating of those models is the work-intensive acquisition of specific cutting forces for oblique cutting. Further, the acquisition of specific cutting forces for different tool and workpiece combinations requires a great number of cutting experiments and much analytical work. In modeling of multidirectional layered materials also the non-homogeneities in materials must be considered making the determination of specific cutting forces even more exacting.

Models for simulating of cutting forces in orthogonal cutting of layered laminates with different directions of fibres [4, 18, 19] and quite a few models for prediction of cutting forces in helical end milling of metals are available. For example, Kline [20] created a cutting force model by dividing the helical end mill in axial direction into differentially thin elements. For each element, he calculated the differential cutting force as the product of specific cutting force and uncut chip cross-section area. With the sum of differential cutting forces for the entire cutting edge he then determined the total cutting force on the tool.

Zhang *et al*. [21] developed a stochastic model of cutting forces in milling of fibre-reinforced ceramic matrix composites. In this model, the cutting forces are modeled by combining the simultaneous influences of randomly distributed carbon fibres and stochastic deterioration of tool wear. Grdisek *et al*. [22] created a generalized prediction model considering the chip and tool geometry, cutting parameters and specific cutting forces determined by a special method from orthogonal cutting data. Wang *et al*. [23] developed a novel analytic cutting force model of helical milling of titanium alloy. Liu *et al*. [24] developed a cutting force model to predict the cutting forces and torque during helical milling of AISI D2 steel. In the recent years, the artificial neural networks (ANN) for modelling of the milling process have become popular. Zuperl *et al*. [25] used backpropagation ANN for modelling of cutting forces in ball-end milling based on a set of input cutting conditions. Aykut *et al*. [26] applied ANN for predicting cutting forces in face milling of satellite Co-based alloy under dry conditions. El-Mounayri *et al*. [27] introduced a radial basis model for predicting cutting forces in a ball-end milling process. Al-Zubaidi *et al.* in his paper [28] reviewed the previous studies and investigations on the application of artificial neural network in modeling of milling processes.

Balasubramanian *et al*. [29] performed analysis of cutting forces in helical ball end milling of Ti-6Al-4V alloys using deep neural network. On the basis of the results obtained, he concluded that the accuracy of the predicted forces was more than sufficient for any practical purpose.

The models based on neural networks prove to be very accurate in predicting by searching for correlations between cutting parameters and cutting forces, whereas they are not successful in predicting cutting forces on the basis of different properties of workpiece material. Our paper discusses the generalized neuro-mechanistic model for accurate prediction of cutting forces in helical end-milling of multidirectional layered materials. The generalized model consists of a mechanistic prediction model of cutting forces for complex cutting tool geometry and an artificial neural network for prediction of specific cutting forces of a particular layer.

The relevant scientific contribution of this paper is the presented methodology to build a predictive cutting force model for edge milling of multidirectional layered materials with complex cutting tool geometries. The methodology is not limited to one cutting tool; it can be extended to all other complex cutting tools where the instantaneous uncut chip thickness and direction of the layer deposition can be determined.

The paper is organized as follows: Section 2 presents the methodology of creating of combined neuro-mechanistic model for prediction of cutting forces in helical end-milling of multidirectional layered material. Subection 2.1 outlines an overview of the proposed cutting force model. Subection 2.2 presents the developed mechanistic model for prediction of cutting forces by considering the geometry of the helical end milling cutter, instantaneous chip thickness and direction of depositing of individual layers of multi-layer material. Subsection 2.3 describes the artificial neural network based modeling and predicting of specific cutting forces for each direction of deposition of individual layer of layered material. Subsection 2.4 outlines the experimental set-up. In Section 3 the results of comparison of the model prediction with experimental data are analyzed. Section 4 gives the concluding remarks.

2. Materials and methods

A quantitative study design was undertaken in three phases. In the first phase, edge milling of metal materials layered in different directions was executed in order to obtain orthogonal data base (milling force data) for determining specific cutting forces. Mechanistic technique was employed to predict specific cutting forces. In the second phase, an artificial neural network was built to estimate specific cutting forces. In the third phase, a generalized cutting force model was developed based on mechanistic modeling technique [17, 24]. The model was verified by comparing predicted and experimentally acquired values. The average percentage error (APE) was employed to evaluate the accuracy of the neural and cutting force model.

2.1 Overview of proposed cutting force model for multidirectional layered material

Hereinafter, a combined neural-mechanistic model for prediction of cutting forces in helical end-milling of multidirectional layered metal material is presented. The model is capable of predicting the cutting forces for selected combination of cutting parameters, immersion angle and direction of deposition of individual workpiece layers. For creation of the model, the mechanistic modeling technique of complex tool geometry, dividing the helical tool cutting edge in axial direction into a great number of equal differential elements with angle offset, is used. By the use of trained artificial neural network the radial and tangential cutting force coefficients (K_r, K_t) are evaluated for each element. Based on evaluated instantaneous coefficients K_r and K_t the radial dF_r and tangential dF_t differential forces for each individual differential element are calculated. In the end, the total force on the cutting tooth is calculated by integrating differential forces on all elements of the cutting edge. The force on tool is determined by the sum of cutting forces on all tool cutting edges.

2.2 Creation of cutting force model for helical end mill

Cutting forces are calculated for the end mill with helix angle β, diameter D and number of cutting edges N. The milling cutter with designated cutting force direction and differential segments

is shown in Fig. 1. The two elementary forces dF_t and dF_r on the differential element L are determined on the basic of instantaneous values K_r and K_t, instantaneous uncut chip thickness h_L and milling width. Tangential force dF_t and radial force dF_r acting on the differential element L of dz height are calculated according to Eqs. 1 and 2:

$$dF_r(\phi_L, z) = \left[K_{re} + K_r \cdot h_L(\phi_L, z)\right] \cdot dz \tag{1}$$

$$dF_t(\phi_L, z) = \left[K_{te} + K_t \cdot h_L(\phi_L, z)\right] \cdot dz \tag{2}$$

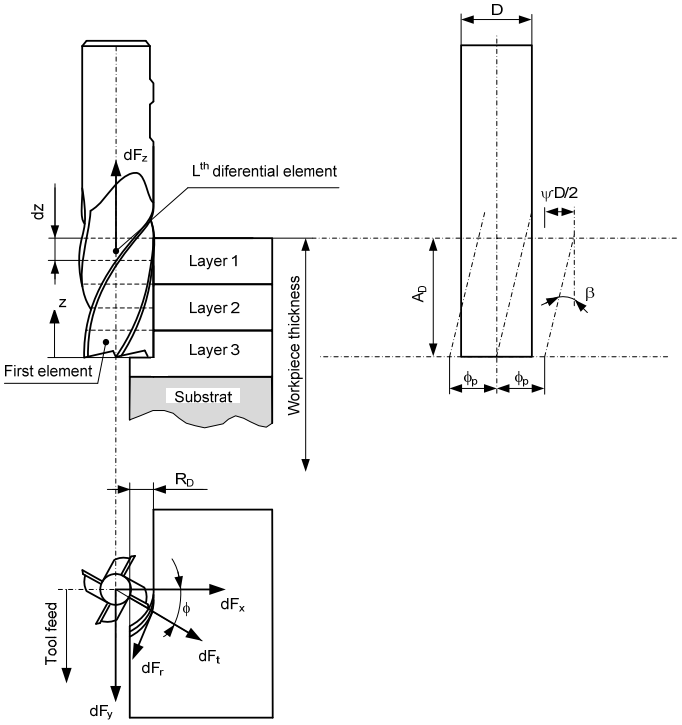

Fig. 1 Geometry of helical end milling of multidirectional layered material with relevant cutting forces and tool dissection into differential elements

The immersion (engagement) angle for differential element L on tooth j at an axial depth of cut z is calculated according to:

$$\phi_L(z) = \phi + j\phi_p - \lambda \tag{3}$$

In the calculation, it is assumed that the bottom part of the cutting edge $j = 0$ has reference immersion angle ϕ. The bottom end points of the other cutting edges are offset from reference cutting edge by angle $\phi_p = 2\pi/\mathrm{N}$. This relation is written with Eq. 4:

$$\phi_j(z = 0) = \phi + j\phi_p; \quad j = 0, 1, \ldots, (N-1) \tag{4}$$

where ϕ_p is the angular pitch of cutting edge. Lag angle for differential element L for axial cut depth z is calculated Eq. 5:

$$\lambda = \frac{2\tan\beta}{D} \cdot z \tag{5}$$

h_L for the differential element is calculated according to Eq. 6.

$$h_L(\phi_L, z) = f_z \cdot \sin\phi_L; \quad f_z = \frac{f}{n \cdot N} \tag{6}$$

where f is the feed rate and n is the rotational tool speed.

The cutting force components with zero chip thickness are designated as K_{te} and K_{re}.

The effect of cutting tool wear is not considered because sharpened tool is used for each pass.

By considering the cutting trigonometry the differential axial cutting force dF_a for L-th differential element is determined on the basis of dF_t and dF_r according to Eq. 7:

$$h_L(\varphi_L, z) = f_z \cdot \sin \phi_L dF_a(\varphi_L, z) = \frac{dF_r(\sin\beta - \cos\beta \cdot \sin\alpha_n \cdot \tan\eta) - dF_t \cdot \cos\alpha_n \cdot \tan\eta}{\sin\beta \cdot \sin\alpha_n \cdot \tan\eta + \cos\beta} \tag{7}$$

where β is the inclination angle of cutting edge, α_n the relief angle and η is the rake angle.
The radial and tangential coefficient of cutting force depend on the direction of layer deposition of layered material and uncut chip thickness determined for the instantaneous engagement angle ϕ_L according to Eq. 6.

The angle of instantaneous direction of deposition of layers of layered material for differential element L is determined according to Eq. 8:

$$\theta_L = \begin{cases} \psi - \phi_L & 0 \le \phi_L < \psi \\ 180 - (\phi_L - \psi) & \phi_L > \psi \\ 180 - \psi & \psi = 0 \end{cases} \tag{8}$$

The angle of deposition of a gradient layer of material is designated ψ.

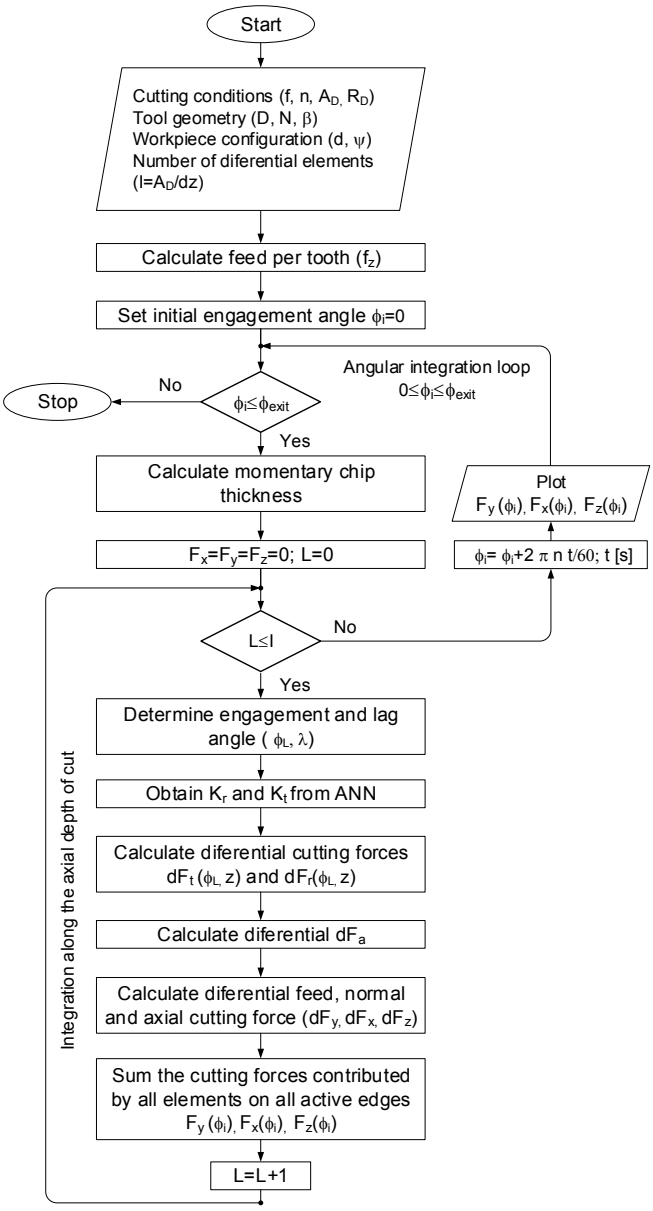

Fig. 2 Algorithm for prediction of cutting forces in helical end milling

Transformation of elementary force dF_r and dF_t into differential feeding force dF_y and normal force dF_x by taking into account the cutting trigonometry is determined according to following equations:

$$dF_x(\phi_L, z) = dF_t \cdot \cos\phi_L(z) - dF_r \cdot \sin\phi_L(z) \tag{9}$$

$$dF_y(\phi_L, z) = dF_t \cdot \sin\phi_L(z) + dF_r \cdot \cos\phi_L(z) \tag{10}$$

$$dF_z(\phi_L, z) = dF_a \tag{11}$$

By integrating the differential forces on the active part of cutting edge (from 0 to A_D) the total cutting force of one cutting edge j is determined. Total cutting forces generated by the tool are determined by the addition of cutting forces on all differential elements of cutting edges. The following expressions are used:

$$F_x(\phi_i) = \sum_{j=0}^{N-1} \sum_{z=0}^{A_D} dF_x; \quad F_y(\phi_i) = \sum_{\substack{j=0 \\ 0 \le \phi_i \le \phi_{exit}}}^{N-1} \sum_{z=0}^{A_D} dF_y; \quad F_z(\phi_i) = \sum_{j=0}^{N-1} \sum_{z=0}^{A_D} dF_z; \tag{12}$$

Fig. 2 shows the algorithm for prediction of cutting forces in milling with helical end milling cutter.

2.3 Neural model of specific cutting forces for unidirectional layered material

This chapter presents the methodology of modelling and predicting of specific cutting forces for unidirectional layered metal material by the use of ANN. Specific cutting force in milling of multi-layer materials depends on the direction of deposition of individual layers, instantaneous chip thickness, cutting speed and tool wear. For a certain pair tool-workpiece the specific cutting force links the cutting parameters to relevant radial and tangential cutting force.

For the individual deposited metal layer of material with defined instantaneous direction of deposition θ its amplitude is calculated according to the following expressions:

$$K_r(n, f, \theta, h) = \frac{F_r(n,f,\theta,h)}{A_D \cdot h(\phi)}; \qquad K_t(n, f, \theta, h) = \frac{F_t(n,f,\theta,h)}{A_D \cdot h(\phi)} \tag{13}$$

In the equation, F_r and F_t are measured cutting forces, the expression in the denominator is the calculated uncut chip area. The experimental data set for calculation of specific cutting forces is obtained by measurement of cutting forces in milling of multi-layer metal workpieces. All layers of the individual workpieces were made with equal direction of deposition.

To train, validate and test the neural model, a total of 54 cutting experiments with three spindle speed levels, three feed rate levels, two axial depth of cutting levels and three different workpiece configurations were conducted.

The data set used for training, validating and testing the neural model consists of 1890 data points. The total data set was split into input and output subsets. The input subset consists of spindle speed n, feed rate f, axial depth of cutting A_D, radial depth of cutting R_D, the direction of the material layer deposition ψ, uncut chip thickness h and hardness of the machined material HV. The output set consists of radial and tangential specific cutting forces.

Further, the total data was randomly divided into training/validation (1260 data points) and testing data subsets (630 data points). A ten-fold cross-validation is used to validate the ANN model. Therefore, 1260 data points were randomly partitioned into 10 equal blocks (folds). Then, ANN models were systematically trained on 9 folds and validated on the remaining fold; the cross-validation process was repeated 10 times. The prediction errors of the trained ANN models were averaged and 95 % confidence interval was determined. After the validation process, a subset of 1260 data points was used to train a new ANN model. Finally, a testing data subset (630 data points) was used to test the developed ANN model.

To evaluate the accuracy of the created models, the average percentage error (APE) calculated according to Eq. 14 is used:

$$APE = \left(\sum_{i=1}^{n} \frac{|K_{target,i} - K_{predicted,i}|}{K_{target,i}} \cdot 100\ \% \right) / n \tag{14}$$

where $K_{target,i}$ is the experimentally determined specific cutting force component, $K_{predicted,i}$ is predicted specific cutting force component in radial and tangential direction generated by ANN and n is the number of testing data points.

For modeling, a four-layer feed forward ANN with backpropagation learning algorithm is used. The rate of training 0.12 and the momentum rate 0.08 are selected for training, while for the transfer of signals between neurons the arctan transfer function is chosen. The input vector of neural network consists of spindle speed n, feed rate f, axial depth of cutting A_D, radial depth of cutting R_D, the direction of the material layer deposition ψ, uncut chip thickness h and hardness of the machined material HV. The value HV did not change in the machining experiment. The output vector ANN consists of radial and tangential specific cutting forces. The ANN architecture shown in Fig. 3 and the optimum training parameters were determined through simulations. The ANN training process was completed, when 8500 iterations of training had been performed or when the prediction error has fallen below the pre-defined limit value (0.01).

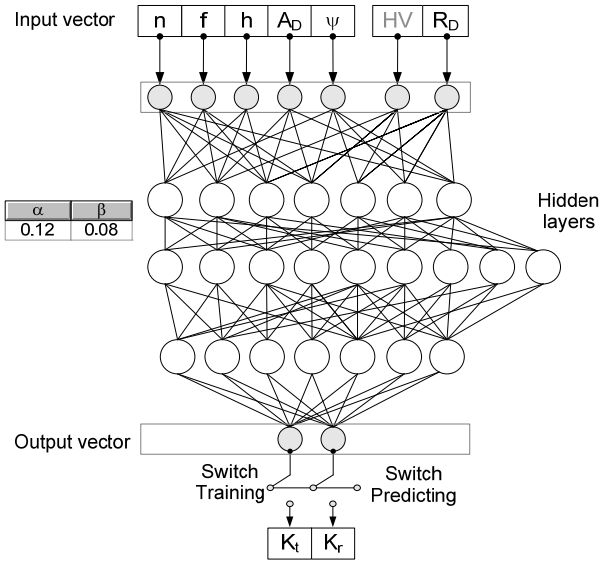

Fig. 3 Detailed structure of ANN used for prediction of components of specific cutting forces depending on material layer deposition direction

2.4 Experimental set-up

To build the cutting force model, a set of machining experiments was performed on the Heller BEA01 milling machine according to the experimental plan. Cutting conditions of performed expriments are described in Table 1.

The orthogonal milling experiments with cutting conditions described in Table 1 have been carried out in order to train and test the ANN model. For determinig the specific cutting forces the stright one tooth cutting tool with a diameter of 16 mm was used. The carbide tool had 3.8° rake angle. Cooling-lubricating agents were not used.

Four complex milling experiments with the same cutting conditions have been carried out in order to obtain the data for verifying the developed generalized neuro-mechanistic model. The model was verified for a segmented helical cutting tool in edge milling of unidirectional and multidirectional workpieces. In these experiments the carbide helical cutting tools with a diameter of 8.5 mm and two flutes were used. The tool from sintered tungsten carbide had 27.3° helix angle and 4.28° rake angle. Cutting edges had PVD-TiAlN coating and hardness of 1820 HV. Cooling-lubricating agents were not used. In all helical milling experiments the same tool rotational frequency 3800 min^{-1} and the same feed rate 200 m/min were selected. The cut depth A_D was adjusted to 1.8 mm and the radial cut depth R_D to 0.5 mm.

Table 1 Cutting conditions of performed machining experiments and material layer deposition directions

Parameter	Orthogonal milling	Helical milling
n [min^{-1}]	3500, 3800, 4100	3800
f [m/min]	200, 250, 300	200
R_D [mm]	1	0.5
A_D [mm]	1.6, 1.8	1.8
D [mm]	16	5.5
Layer depositing direction ψ [^{o}]	90, 180, 135	90, 180, 135, 90/135/180
Number of teeth	1	2
Helix angle [^{o}]	0	27.3
Radial angle [^{o}]	3.8	4.28

Three cutting force components were measured with Kistler piezo-electric dynamometer. The signals of the measured forces were processed with dual mode charge amplifier and low pass filter of 2 kHz cut-off frequency to eliminate noises induced by vibrations of adjacent systems. Adequacy of frequency Bandwidth of dynamometer for all cutting force frequencies in the experiment was confirmed by calculations. Dynamic compensation of measured cutting forces was not employed at low tooth frequencies. Measured signals were transferred to data acquisition with Labview software.

Workpiece of 50 mm length, 15 mm width and 21.8 mm height was clamped to the dynamometer. Two types of workpieces shown in Fig. 4 were used in machining experiments. The first, i.e. unidirectional workpiece type (Fig. 4a) was made from 16MnCr5 basic substrate and several stainless steel (316L) layers with a singular 0.6 mm thickness. All gradient layers were deposited in the same direction. Identical workpieces, properly machined and rotated on Z axis in respect to feed direction for 90°, 135° and 180°, were used in orthogonal milling experiments.

The other, i.e. multidirectional workpiece type (Fig. 4b) was used only in complex helical milling experiment. It was made from a 16MnCr5 basic substrate and three stainless steel (316L) layers deposited in different directions. Each new layer was deposited at 45° angle with respect to the direction of deposition of previous layer. Thus, individual layers were deposited at 90°, 135° and 180° angles. Thickness of individual layers made was 0.6 mm with measured hardness 288 HV. Overlapping of laser trajectories was adjusted to 40 %. Diameter of the effective laser beam was 0.9 mm.

Fig. 4 shows the structure and orientation of used test workpieces in machining experiments.

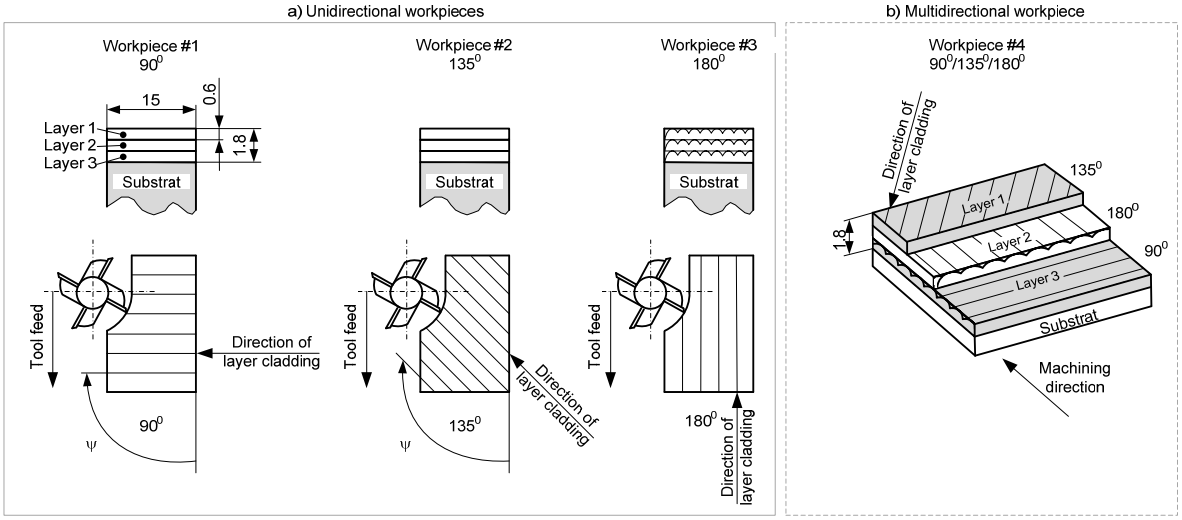

Fig. 4 Structure and position of used unidirectional and/or multidirectional multi-layer workpieces in machining experiments

3. Results and discussion

Many experimental tests with different cutting conditions have been carried out in order to validate the developed generalized neuro-mechanistic model.

A sample of predicted and measured cutting forces in helical milling of unidirectional and multidirectional layered metal material is shown in Figs. 5 and 6. Samples of force values in normal, feed and axial direction are shown diagrammatically depending on the engagement angle. The measured signals of cutting forces, representing the average value of 3 measurements, are represented with full line and predicted values with dashed line. From the flow of cutting force signals it is possible to discern an obvious peak of the cutting force with the tip corresponding to one cutting-off cycle of one cutting tool edge. The cutting force peak results from the increase of chip cross-sectional area on the cutting edge from 0 upon the entry of the cutting edge into material up to maximum value upon the exit of the cutting edge from workpiece. The value and form of the cutting force signal are affected by the layer deposition on the multi-layer material. The instantaneous deposition direction relative to the tool cutting edge changes with the engagement angle.

From the flow of cutting force signals in Fig. 5 it can be discerned that the cutting force values in milling of multi-layer stainless steel with 90° deposition direction are greater than when milling the material with 180° deposition direction. Also a smoother flow of cutting force signals with fewer fluctuations can be discerned. Contacts between deposited layers contribute to formation of very small broken chips. The increase of the deposition direction angle from 90° toward 135° results in strong increase of cutting force fluctuations and magnitude. Most unfavourable cutting forces occur in machining the material with deposition direction 135° (Fig. 6a), where a slightly greater chip cross sectional area of incorrect shapes and from time to time partly continuous appear. Bad cutting conditions might be ascribed to sticking of the cutting edge tip between individual deposited layers. The cutting force magnitudes in milling of unidirectional multi-layer material with deposition direction from 135° towards 180° and partly also fluctuations are decreasing. Greater fluctuations of axial force F_Z can be observed in machining the material with 180° deposition direction (Fig. 5a). More favourable, somewhat larger, broken chips appear. When milling a multidirectional three-layer workpiece (90°/180°/135°) two distinct cutting force tops (Fig. 6b) can be observed. They result from great changes of instantaneous directions of deposited layers on the tool cutting edge, when it passes between individual stainless steel layers. Because of the low $R_{D,}$ only one cutting edge cuts at a time. At the beginning of tool rotation, the tool cutting edge moves vertically on the entire thickness of layer 3. Afterwards, it passes over the layer 2 and, in the end, it gets out of the layer 1 at engagement angle 25°. During gradual cutting of the lowest layer 3 with 90° deposition direction the first peak of all three cutting force components (Fig. 6b) occurs.

A decrease of cutting forces, coinciding with cutting of the middle layer with 180° deposition direction, follows. During cutting of the highest layer with 135° deposition direction the second, somewhat smaller, peak of the cutting force component occurs. The greatest magnitudes and fluctuations of cutting force values occur when machining this layer particularly because of greater cross and unfavourable form of the chip and rough tearing of the chip from workpiece. Machining of the highest layer with 130° deposition direction contributes most to the total cutting force shown in Fig. 6b and machining of the middle layer with 180° deposition direction contributes least. The sizes, sequences and distances of peaks of measures cutting forces depend on the sequence and thicknesses of deposited layers constituting the multidirectional multi-layer metal material.

Comparison between measured and predicted forces for helical end milling of unidirectional multi-layer material is shown in Figs. 5a, 5b and 6a. Fig. 6b shows the comparison between measured and predicted forces for milling of multi-layer material with layer deposition directions (90°/180°/135°). Results in Figs. 5 and 6 witness that the predicted force values agree well with experimentally obtained values in milling of 180° and 135° unidirectional multi-layer workpiece. A slightly smaller agreement of predicted and measured forces is discerned in milling of unidirectional workpiece with 90° direction of laser-deposited layers.

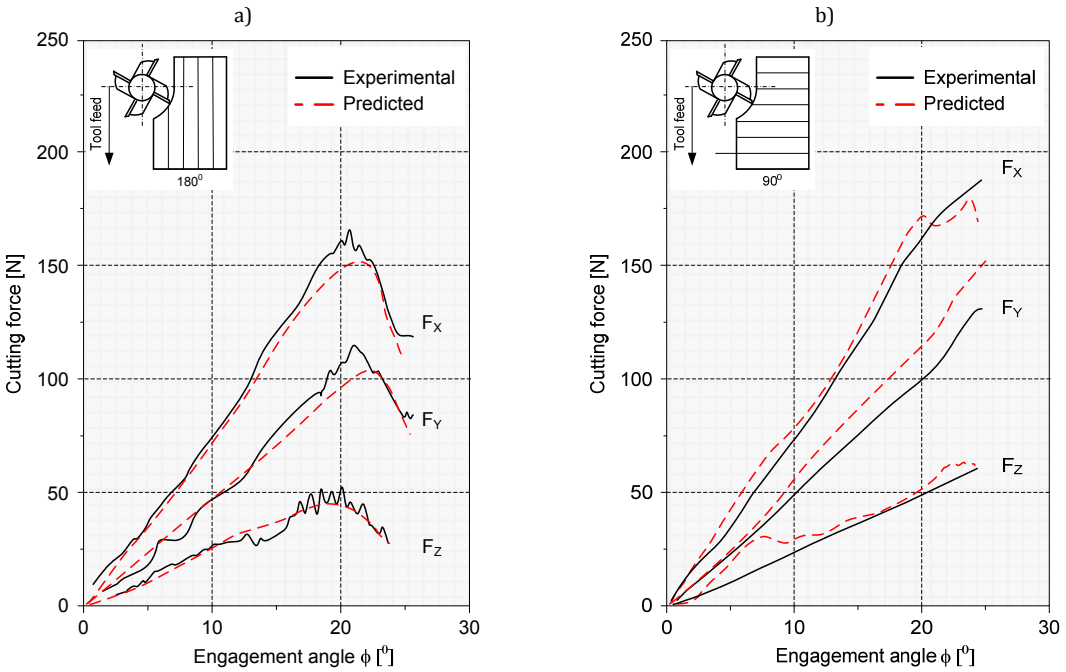

Fig. 5 Comparison between experimental and predicted cutting forces for unidirectional three-layer metal material with: a) with 180⁰ direction of layer deposition b) with 90⁰ direction of layer deposition

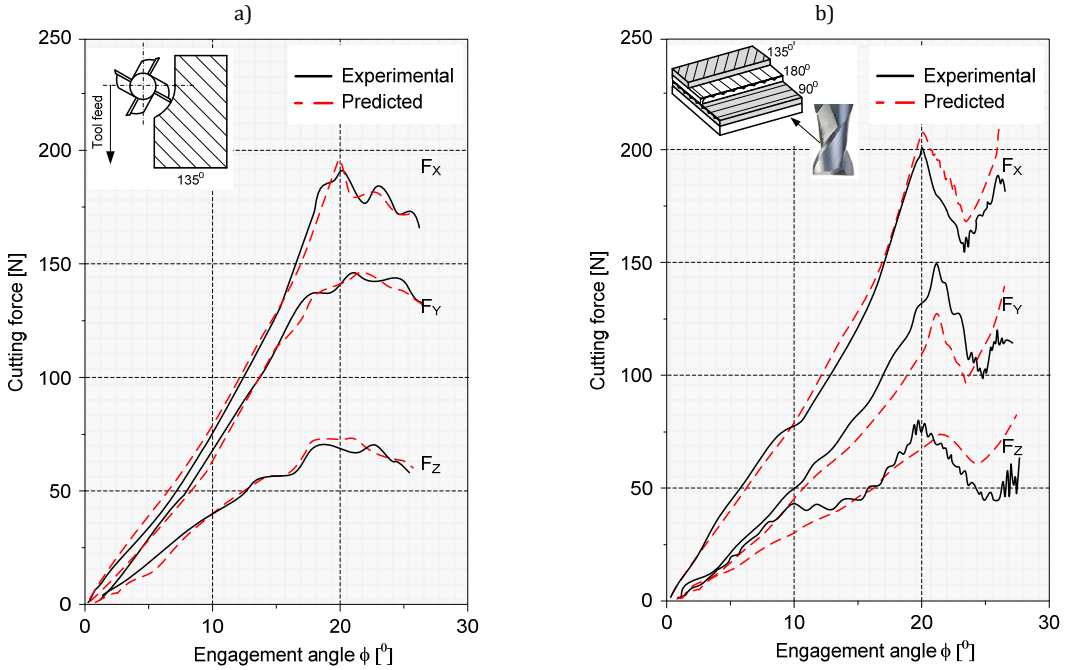

Fig. 6 Comparison between experimental and predicted cutting forces for unidirectional and multidirectional three-layer metal material: a) with 135⁰ direction of layer deposition b) with 90⁰/180⁰/135⁰ directions of layers deposition

The greatest deviation between the model predictions and experimental values of forces occurs in milling of multidirectional workpiece with layer deposition directions (90°/180°/135°). The results differ as follows: from 2.9 % to 8.6 % for F_x, from 3.6 % to 11.7 % for F_y and from 3.6 % to 16.1 % for F_z.

The results in Figs. 5 and 6 show that the developed model appropriately predicts the general course of cutting forces in milling of multi-layer materials.

Table 2 Accuracy of ANN prediction model

ANN	K_r	K_t
APE [%]; Training set	4.29	4.25
APE [%]; Testing set	5.21	3.55

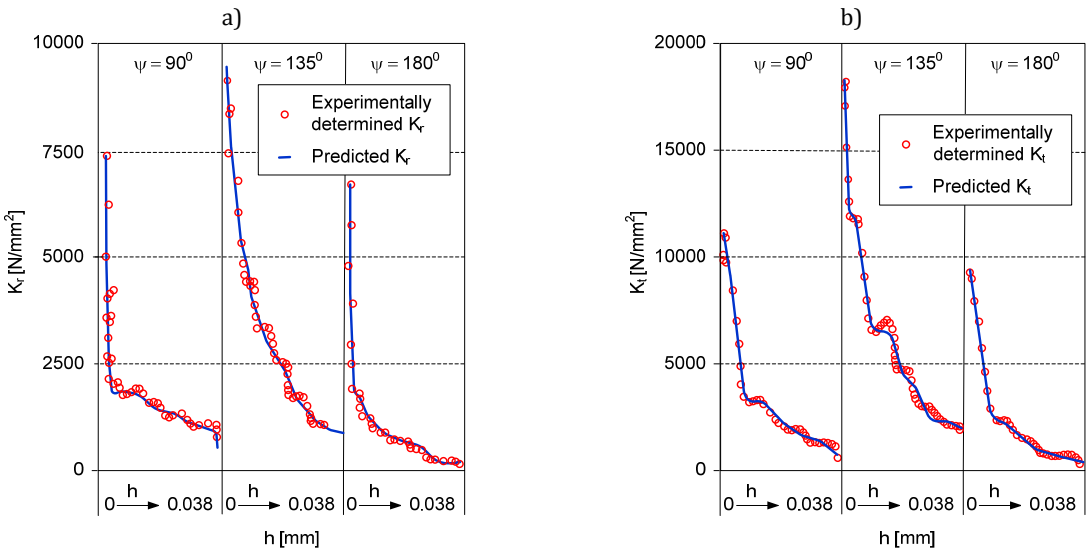

Fig. 7 Comparison of K_r and/or K_t predicted by neural model and obtained experimentally with four different directions of layer deposition; f = 200 m/min, n = 3800 min^{-1}

The accuracy of the ANN model for predicting specific cutting forces was analysed using the APE method. The results of analysis of the model capacity are given in Table 2. The uncertainty of the predicted results, obtained from the ten-fold cross-validation, can be characterized as small, consequently it was concluded that the ANN adequately predicted K_r and K_t. The maximal prediction error of the ANN model is 5.21 % for K_r, and 3.55 % for K_t with a 95 % confidence interval. A part of predicted values K_t and K_r depending on the layer deposition angle and uncut chip thickness is presented in two graphs in Fig. 7. Both graphs show that the predicted values of specific components of cutting forces in radial and tangential direction strongly agree with experimentally obtained values. The two specific cutting forces decrease with the increase of the engagement angle and/or instantaneous uncut chip thickness. The greatest values are reached with layer deposition angle 135°.

4. Conclusion

The paper presents a combined neural-mechanistic model of the process of helical milling of multidirectional layered metal materials.

For creation of model the mechanistic technique of cutting force prediction was used by dividing the helical end mill into a series of differentially thin axial elements with oblique cutting edges and calculating the differential cutting force for each element. To that end, it uses specific cutting forces predicted by the artificial neural network and incorporates in the calculation the deposition direction of individual layer of multidirectional layered metal material. The total cutting force for any immersion tool angle is calculated by integrating the differential cutting forces on the height of the tool cutting edge in contact with the multi-layer workpiece.

The model is capable of predicting the cutting forces in milling of multidirectional and unidirectional metal materials with complex geometry tools.

Many cutting experiments have been carried out to validate the developed model. The following conclusions can be drawn from these experiments:

- The magnitude of cutting forces in milling of multidirectional layered metal material is affected by the layer deposition direction and immersion angle of cutting tool determining the instantaneous cross-section of the chip.
- The developed model appropriately predicts the general course of cutting forces during milling of multidirectional metal materials. It can be recapitulated that the model created is generally efficient (valid) for any combination of cutting parameters and direction of workpiece layer deposition.
- Accuracy of the model prepared is high in milling of unidirectional metal materials and slightly worse in milling of the workpiece with multidirectional laser deposited layers.
- The neural network incorporated in the model predicts the specific cutting forces for any instantaneous direction of deposition of material layers, therefore the proposed model is widely applicable and capable of simulating the cutting forces on the helical milling tool for multidirectional layered metal material.
- The predicted cutting force values agree well with experimentally obtained values in milling 180° and 135° unidirectional multi-layer workpiece. A slightly smaller agreement between predicted and measured forces is found in milling unidirectional workpiece with 90° direction of layer deposition. These minor errors are not random. They might appear due to the failure to take into account the entire cutting tool geometry when calculating the specific cutting forces.
- The results differ as follows: from 2.9 % to 8.6 % for F_x, from 3.6 % to 11.7 % for F_y and from 3.6 % to 16.1 % for F_z.
- The maximum percentage prediction cutting force is found to be less than 16.1 % for all the cases tested.

References

[1] Mahmoud, E.R.I. (2015). Characterizations of 304 stainless steel laser cladded with titanium carbide particles, *Advances in Production Engineering & Management*, Vol. 10, No. 3, 115-124, doi: 10.14743/apem2015.3.196.

[2] Tabernero, I., Lamikiz, A., Martínez, S., Ukar, E., Figueras, J. (2011). Evaluation of the mechanical properties of Inconel 718 components built by laser cladding, *International Journal of Machine Tools and Manufacture*, Vol. 51, No. 6, 465-470, doi: 10.1016/j.ijmachtools.2011.02.003.

[3] Jia, Z.-Y., Ge, J., Ma, J.-W., Gao, Y.-Y., Liu, Z. (2016). A new cutting force prediction method in ball-end milling based on material properties for difficult-to-machine materials, *The International Journal of Advanced Manufacturing Technology,* Vol. 86, No. 9-12, 2807-2822, doi: 10.1007/s00170-016-8351-8.

[4] Sheikh-Ahmad, J., He, Y., Qin, L. (2019). Cutting force prediction in milling CFRPs with complex cutter geometries, *Journal of Manufacturing Processes,* Vol. 45, 720-731, doi: 10.1016/j.jmapro.2019.08.009.

[5] M'Saoubi, R., Axinte, D., Soo, S.L., Nobel, C., Attia, H., Kappmeyer, G., Engin, S., Sim, W.-M. (2015). High performance cutting of advanced aerospace alloys and composite materials, *CIRP Annals,* Vol. 64, No. 2, 557-580, doi: 10.1016/j.cirp.2015.05.002.

[6] Hojati, F., Daneshi, A., Soltani, B., Azarhoushang, B., Biermann, D. (2020). Study on machinability of additively manufactured and conventional titanium alloys in micro-milling process, *Precision Engineering*, Vol. 62, No. 1-9, doi: 10.1016/j.precisioneng.2019.11.002.

[7] Bonaiti, G., Parenti, P., Annoni, M., Kapoor, S. (2017). Micro-milling machinability of DED additive titanium Ti-6Al-4V, *Procedia Manufacturing,* Vol. 10, 497-509, doi: 10.1016/j.promfg.2017.07.104.

[8] Montevecchi, F., Grossi, N., Takagi, H., Scippa, A., Sasahara, H., Campatelli, G. (2016). Cutting forces analysis in additive manufactured AISI H13 alloy, *Procedia CIRP*, Vol. 46, 476-479, doi: 10.1016/j.procir.2016.04.034.

[9] Song, G., Sui, S., Tang, L. (2015). Precision prediction of cutting force in oblique cutting operation, *The International Journal of Advanced Manufacturing Technology*, Vol. 81, No. 1-4, 553-562, doi: 10.1007/s00170-015-7206-z.

[10] Yang, L., Zheng, M.L. (2017). Simulation and analysis of ball-end milling of panel moulds based on Deform 3D, *International Journal of Simulation Modelling*, Vol. 16, No. 2, 343-356, doi: 10.2507/IJSIMM16(2)CO9.

[11] Sun, Y., Guo, Q. (2011). Numerical simulation and prediction of cutting forces in five-axis milling processes with cutter run-out, *International Journal of Machine Tools and Manufacture*, Vol. 51, No. 10-11, 806-815, doi: 10.1016/j.ijmachtools.2011.07.003.

[12] Omar, O.E.E.K., El-Wardany, T., Ng, E., Elbestawi, M.A. (2007). An improved cutting force and surface topography prediction model in end milling, *International Journal of Machine Tools and Manufacture*, Vol. 47, No. 7-8, 1263-1275, doi: 10.1016/j.ijmachtools.2006.08.021.

[13] Tuysuz, O., Altintas, Y., Feng, H.-Y. (2013). Prediction of cutting forces in three and five-axis ball-end milling with tool indentation effect, *International Journal of Machine Tools and Manufacture*, Vol. 66, 66-81, doi: 10.1016/j.ijmachtools.2012.12.002.

[14] Qu, S., Zhao, J., Wang, T., Tian, F. (2015). Improved method to predict cutting force in end milling considering cutting process dynamics, *The International Journal of Advanced Manufacturing Technology*, Vol. 78, No. 9-12, 1501-1510, doi: 10.1007/s00170-014-6731-5.
[15] Cao, Q., Zhao, J., Li, Y., Zhu, L. (2013). The effects of cutter eccentricity on the cutting force in the ball-end finish milling, *The International Journal of Advanced Manufacturing Technology*, Vol. 69, No. 9-12, 2843-2849, doi: 10.1007/s00170-013-5205-5.
[16] Daoud, M., Chatelain, J.F., Bouzid, A. (2017). Effect of rake angle-based Johnson-Cook material constants on the prediction of residual stresses and temperatures induced in Al2024-T3 machining, *International Journal of Mechanical Sciences*, Vol. 122, 392-404, doi: 10.1016/j.ijmecsci.2017.01.020.
[17] Li, Y., Yang, Z.J., Chen, C., Song, Y.X., Zhang, J.J., Du, D.W. (2018). An integral algorithm for instantaneous uncut chip thickness measuring in the milling process, *Advances in Production Engineering & Management,* Vol. 13, No. 3, 297-306, doi: 10.14743/apem2018.3.291.
[18] Karpat, Y., Polat, N. (2013). Mechanistic force modeling for milling of carbon fiber reinforced polymers with double helix tools, *CIRP Annals*, Vol. 62, No. 1, 95-98, doi: 10.1016/j.cirp.2013.03.105.
[19] Kalla, D., Sheikh-Ahmad, J., Twomey, J. (2010). Prediction of cutting forces in helical end milling fiber reinforced polymers, *International Journal of Machine Tools and Manufacture*, Vol. 50, No. 10, 882-891, doi: 10.1016/j.ijmachtools.2010.06.005.
[20] Kline, W.A., DeVor, R.E., Lindberg, J.R. (1982). The prediction of cutting forces in end milling with application to cornering cuts, *International Journal of Machine Tool Design and Research*, Vol. 22, No. 1, 7-22, doi: 10.1016/0020-7357(82)90016-6.
[21] Zhang, X., Yu, T., Zhao, J. (2020). An analytical approach on stochastic model for cutting force prediction in milling ceramic matrix composites, *International Journal of Mechanical Sciences*, Vol. 168, Article No. 105314, doi: 10.1016/j.ijmecsci.2019.105314.
[22] Gradišek, J., Kalveram, M., Weinert, K. (2004). Mechanistic identification of specific force coefficients for a general end mill, *International Journal of Machine Tools and Manufacture*, Vol. 44, No. 4, 401-414, doi: 10.1016/j.ijmachtools.2003.10.001.
[23] Wang, H., Qin, X., Ren, C., Wang, Q. (2012). Prediction of cutting forces in helical milling process, *The International Journal of Advanced Manufacturing Technology*, Vol. 58, No. 9-12, 849-859, doi: 10.1007/s00170-011-3435-y.
[24] Liu, C., Wang, G., Dargusch, M.S. (2012). Modelling, simulation and experimental investigation of cutting forces during helical milling operations, *The International Journal of Advanced Manufacturing Technology*, Vol. 63, No. 9-12, 839-850, doi: 10.1007/s00170-012-3951-4.
[25] Zuperl, U., Cus, F., Mursec, B., Ploj, T. (2006). A generalized neural network model of ball-end milling force system, *Journal of Materials Processing Technology*, Vol. 175, No. 1-3, 98-108, doi: 10.1016/j.jmatprotec.2005.04.036.
[26] Aykut, Ş., Gölcü, M., Semiz, S., Ergür, H.S. (2007). Modeling of cutting forces as function of cutting parameters for face milling of satellite 6 using an artificial neural network, *Journal of Materials Processing Technology*, Vol. 190, No. 1-3, 199-203, doi: 10.1016/j.jmatprotec.2007.02.045.
[27] El-Mounayri, H., Briceno, J.F., Gadallah, M. (2010). A new artificial neural network approach to modeling ball-end milling, *The International Journal of Advanced Manufacturing Technology*, Vol. 47, No. 5-8, 527-534, doi: 10.1007/s00170-009-2217-2.
[28] Al-Zubaidi, S., Ghani, J.A., Haron, C.H.C. (2011). Application of ANN in milling process: A review, *Modelling and Simulation in Engineering*, Vol. 2011, No. 9, Article ID 696275, doi: 10.1155/2011/696275.
[29] Balasubramanian, A.N., Yadav, N., Tiwari, A. (2020). Analysis of cutting forces in helical ball end milling process using machine learning, *Materials Today: Proceedings,* In press, doi: 10.1016/j.matpr.2020.02.098.